A Study on Properties of Corrosion Fracture Surfaces of GFRP in Synthetic Sea Water

Yon-Jig Kim* and Jae-Kyoo Lim*

(Received June 17, 1996)

In this paper we investigate the stress corrosion cracking (SCC) mechanism and the properties of the corrosion fracture surface of glass fiber reinforced plastics (GFRP) produced by hand lay-up (HLU) in synthetic sea water. The test material is a GFRP with vinylester type epoxy acrylate resin (an unsaturated polyester) as the matrix and chopped strand mat (CSM) type E-glass fiber as the reinforcement. The slow strain rate test (SSRT) was performed on dry and wet specimens in air and sea water. Here the pH concentration of synthetic sea water was controlled to 6.0, 8.2 and 10.0, and the strain rates varied from $1\times10^{-4}(\sec^{-1})$ to 1×10^{-7} $(\sec^{-1})$. The results confirm the fact that in wet specimens tested at a particular strain rate, evidence of SCC such as co-planar, mirror and hackle zone appear. Moreover, stress corrosion of GFRP in sea water was characterised by flat fracture surfaces with only small amounts of fiber pull-out.

Key Words : Glass Fiber Reinforced Plastic, Stress Corrosion Cracking, Co-planar, Mirror Zone, Mist Zone, Hackle Zone, Fiber Pull-Out

1. Introduction

Glass fiber reinforced plastic (GFRP) composites are extensively used with engineering materials in ocean engineering applications such as ships, harbor facilities and floating structures. GFRP must survive in the environment to which they are subjected at least as well as the conventional engineering materials they replace. The conditions are often severe, frequently combining stress and sea water.

In most environments GFRP is reasonably inert, especially when the component is not subjected to service loads. Recently, however, it has been shown that even in an aqueous environment in the presence of a sustained load, stress corrosion cracking (SCC) can occur (Aveston, Kelly and Sillwood, 1980). Therefore, it is expected that failures of GFRP will occur by SCC in sea water, but SCC behavior of GFRP in sea water has not been studied extensively.

The present work is concerned primarily with the effects of pH concentration in sea water on stress corrosion, and is based on the slow strain rate test (SSRT) of GFRP plates. In particular, we investigate the SCC mechanisms and the properties of corrosion fracture surfaces of GFRP in sea water.

* Division of Mechanical Engineering, College of Engineering, Chonbuk National University, 664-14, 1-Ga Dokchin-Dong, Dokchin-Gu, Chonju, Korea, 561-756

2. Experimental Procedure

2.1 Materials

The GFRP plates produced by hand lay-up (HLU)(Milewski and Katz, 1987) were used throughout this investigation. This process was one of the first developed following the perfection and utilization of polyester resins. In the preparation of GFRP, two surface mats (SM) and four chopped strand mats (CSM) were used as the reinforcement, while the matrix was composed of vinylester type epoxy acrylate resin, an unsaturated polyester. The filaments were surface treated

with an epoxy-compatible silane finish by the manufacturer. Any bubbles and voids were eliminated by rolling out. This plate was allowed to sit at room temperature for 24 hours, followed by a post cure of 2 hours at 120(℃). The plate had a final thickness of 3.2(mm) and a fiber content of 30~35(wt.%).

The chemical composition and mechanical properties of E-glass fiber are shown in Table 1.

Table 1 Chemical composition and mechanical properties of E-glass fiber.

SiO_2	Al_2O_3	B_2O_3	CaO,MgO	Na_2O	K_2O	Fe_2O_3	F_2
55.2	14.8	7.3	22.0	0.3	0.2	0.3	0.3

(a) Composition(wt.%)

Filament tensile strength (Kg_f/mm^2)	Strand tensile strength (Kg_f/mm^2)	Coefficient of thermal expansion (10^{-6}/℃)	Young's modulus (Kg_f/mm^2)
370	225	5.0	7700

(b) Mechanical properties(25°C)

2.2 Sea water absorption

Synthetic sea water recommended by ASTM D 1141 was used in this test with pH concentrations of 6.0, 8.2 and 10.0.

The specimens for testing sea water absorption were machined in the form of a bar 76.2(mm) long by 25.4(mm) wide, with the same sheet thickness as prepared above(3.2mm). The specimens were soaked in each synthetic sea water sample at room temperature and weighed at various time intervals to determine the rate of sea water absorption. The sea water absorption rate was not affected by pH concentration in synthetic sea water, and the rate for saturation is 0.45(wt.%) as shown Fig. 1. A more detailed description of the test procedure is given by ASTM D 570.

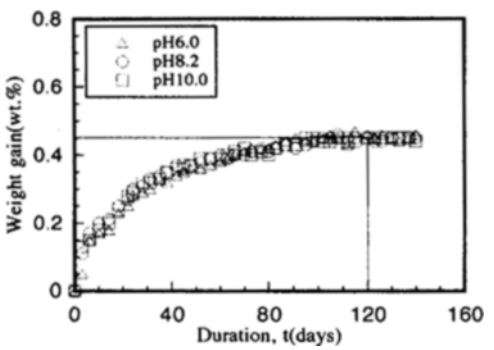

Fig. 1 Diffusion behavior of synthetic sea water into GERP at room temperature.

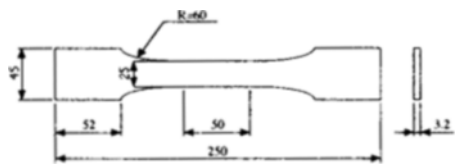

Fig. 2 Dimension of specimen for SSRT(JIS K 7054).

2.3 Specimens

The resulting sheets were finally machined into specimens having the dimensions indicated in Fig. 2 by JIS K 7054. In this test, two types of specimens were used: one is a dry specimen which was cured for 2 hours at 50±3(℃) before test, while the wet specimen was immersed so as to be saturated in synthetic sea water for 4 months. The sea water absorption rate of the wet specimen was 0.45(wt.%).

In this test, each specimen was named as in Table 2 to distinguish the test conditions of GFRP. In this table, the AA condition means that the specimen held in air and tested in air, AS means that the specimen was held in air and tested in synthetic sea water, and SS means that the specimen was immersed and tested in synthetic sea water.

Table 2 The name of specimens tested in each condition.

Environment / Specimen	pH concentration of synthetic sea water used in this test			Air
	pH6.0	pH8.2	pH10.0	
Dry specimen	AS60	AS82	AS10	AA
Wet spcimen	SS60	SS82	SS10	·

2.4 Test method

The slow strain rate tests were carried out in air and synthetic sea water conditions. The strain rates varied from $1\times10^{-4}(sec^{-1})$ to $1\times10^{-7}(sec^{-1})$. However, the sea water was circulated to prevent stagnation, and its pH concentration was measured every 12 hours to ensure that it remain constant.

The fractography of all specimens fractured in air and synthetic sea water was investigated to understand microstructures and SCC mechanisms of GFRP in sea water.

3. Results and Discussion

3.1 Mechanical properties

A typical example of the load-displacement curves obtained from SSRT is shown in Fig. 3, in which the strain rate is $1\times10^{-6}(sec^{-1})$. For the AA case, it is found that the load-displacement curve is approximately linear at first, and that its curve shows small ductile behavior immediately before maximum load (P_{max}). The sudden drop of the curve no longer occurs once its load reaches P_{max}. We believe that this behavior preceding P_{max} is due to a nonlinear relationship between fiber and resin because of the plasticity of the resin. For the AS82 and SS82 cases, however, ductile behavior is less than that of the AA case, and the deterioration of mechanical properties such as maximum load, displacement and fracture strain energy (defined as an area under the curve up to the P_{max}) occurs.

Figure 4 shows the load-displacement curves according to the pH concentration for wet specimens. It can be seen that ductile behavior and mechanical properties decrease with pH concentration.

Consequently, we can describe the variation in properties from the hardness measurement results of the resin according to test environments as shown in Fig. 5. From this figure, we suspect that the ductile behavior before fracture of GFRP is controlled by the extent of the hardening of the resin in synthetic sea water. In general, it has been reported that aromatic groups, in either dihydric alcohol or acid component, promoted increased stiffness and hardness (Dudgeon, 1987). Further study is required in order to understand the hardening of resin in synthetic sea water. We can also expect that the loss of interfacial bond strength occurs at fiber-resin interface. This is due to the discrepancy of contraction between fiber and resin, which causes a deterioration of the mechanical properties of GFRP in synthetic sea water.

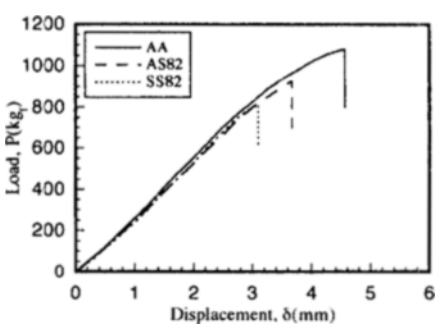

Fig. 3 Load-displacement curves(pH8.2, $1\times10^{6}sec^{-1}$).

3.2 The properties of fracture surface

GFRP composites can fail in many different ways, and both the specific definition of failure and the failure mode depend on the type of composite, the function of the structure, and relevant conditions such as stress and environment. The basis for the SCC process in GFRP is the

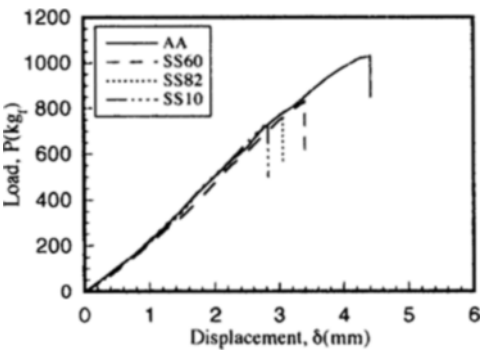

Fig. 4 Load-displacement curves of wet specimens(1×10^{7} sec^{-1}).

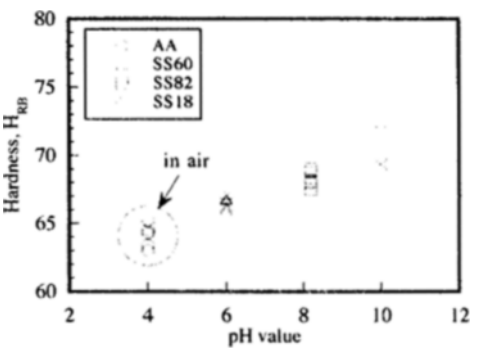

Fig. 5 Relation between hardness of resin and pH value in synthetic sea water(100Kg$_f$).

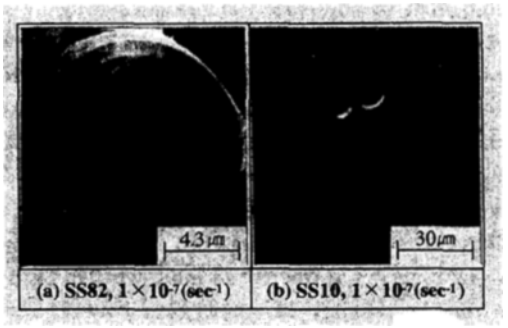

Fig. 6 SEM photographs of co-planar and stress corrosion fiber fracture surface.

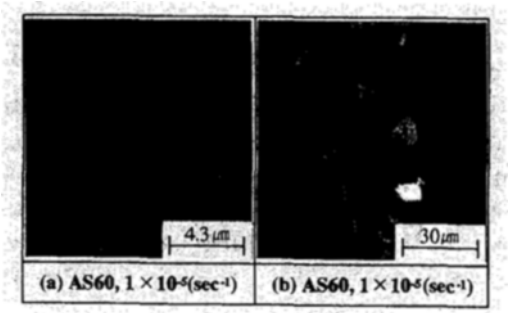

Fig. 7 SEM photographs of fiber pull-out and fiber fracture surface.

degradation of glass fibers by the environment. If stressed glass fibers are exposed to any solution they suffer a SCC process, and the special types of fracture surface in glass fibers will appear.

A typical fiber fracture surface from SCC is shown in Fig. 6(a) and the mirror(A) and hackle zone(B) are observed on the fracture surface. The mirror zone is the initiating point of the SCC for the glass fiber, and the hackle zone produces the rough region, which shows the crack orientation. When this type of fiber fracture occurs, the cracks sweep into the surrounding matrix and the co-planar is produced as shown in Fig. 6(b). For the non-SCC, however, the stress is intensified in the flaws that exist on the surface of glass fibers, and when the stress exceeds the fracture strength of the fibers, the rough fracture surface of the fiber appears. Fracture surfaces of this type are caused by an unstable fracture as shown in Fig. 7(a). This causes a number of fibers to pull-out as shown in Fig. 7(b), because the weak spot on the fiber is not necessarily co-planar with the matrix crack.

In this paper, we have examined the fractographs of GFRP tested in each condition on SCC. From the result, we could not observe evidence of SCC for the AA and AS cases. However, it was observed that SCC occurred in GFRP (SS) at a particular condition. This implies that the occurrence of SCC depends on the amount of sea water absorbed before the test. Figure 8 illustrates a series of scanning electron microscope (SEM) fractographs of glass fibers, ascertaining the probability of SCC. It can be seen that SCC is apt to occur as pH concentration increases in synthetic sea water. The region of SCC failure obtained from the SSRT is shown in Table 3.

Table 3 The situation of SCC occurrence of glass fiber in synthetic sea water.

Strain rate	Dry specimen			Wet specimen		
	AS60	AS82	AS10	SS60	SS82	SS10
$1\times10^{-4}(sec^{-1})$	×	×	×	×	×	×
$1\times10^{-5}(sec^{-1})$	×	×	×	×	×	△
$1\times10^{-6}(sec^{-1})$	×	×	×	×	△	○
$1\times10^{-7}(sec^{-1})$	×	×	×	△	○	○

○: SCC △: quasi-SCC ×: non-SCC

3.3 SCC mechanisms of GFRP in synthetic sea water

The SCC of GFRP in sea water results from the flow of sea water into its components. Sea water absorption by GFRP seems to occur by two processes: one is a resin, the other an interface between fiber and resin. The former can be explained by Fick's law, but the amount of sea water generally absorbed by resin is quite small (Bonniau and Bunsell, 1981). Sea water absorption by GFRP seems to occur mostly through the interface between fiber and resin.

Sea water flows in the weak interface with high speed by a capillary phenomenon. At the interface, sea water decreases the interfacial bond strength and is absorbed on the fiber. For the lowest strain rate, sea water is sufficiently absorbed at the GFRP through the fiber-resin interface, and chemical attack of the fiber proceeds for a fairly long-time. Eventually, stress corrosion cracks form under the combined influ-

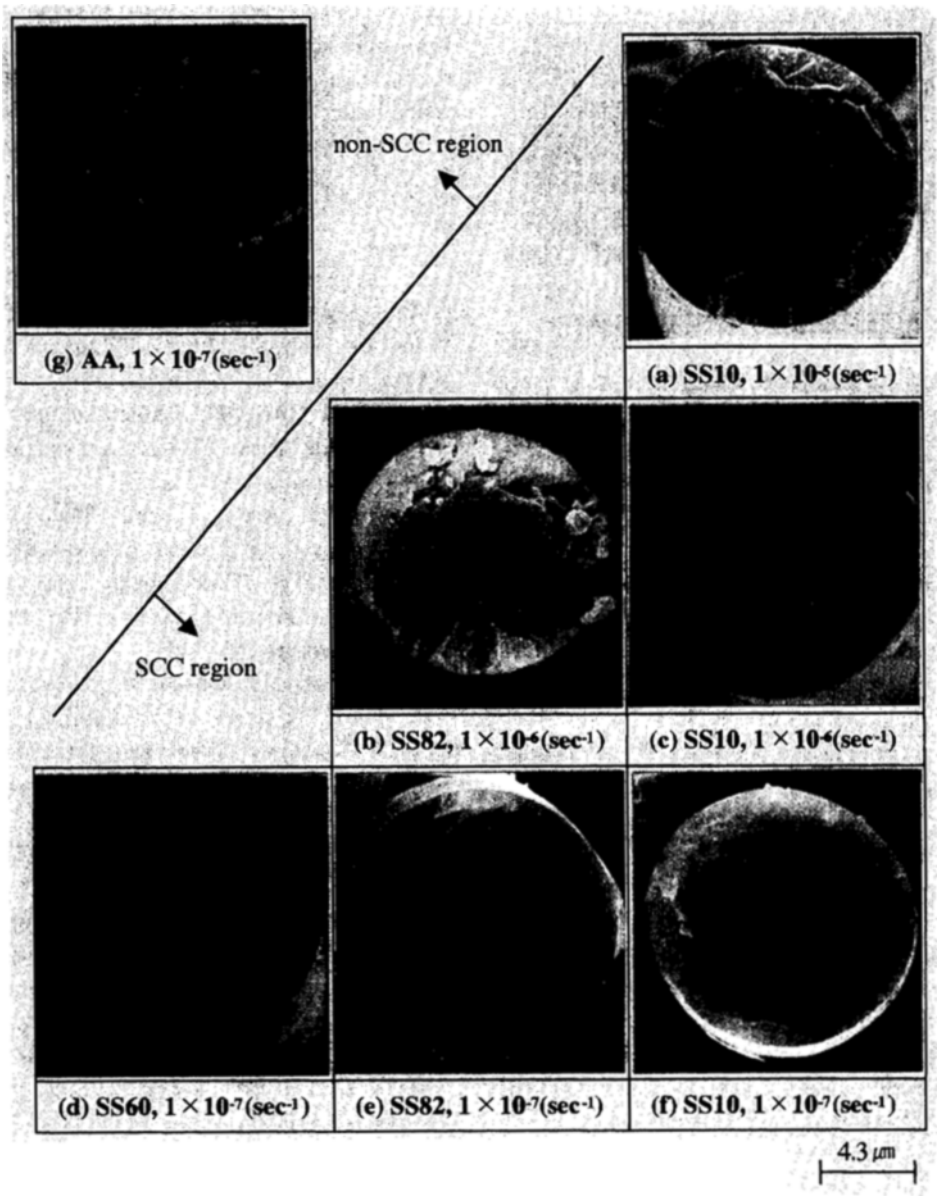

Fig. 8 SEM photographs of fiber fracture surface for AA and SS materials.

ence of stress and sea water, and if the crack tip stress is sufficient, a fracture radiates to the resin. Therefore, fiber fracture occurs at the point of environmental attack, and this produces the characteristic flat fracture surfaces associated with SCC in GFRP as shown in Fig. 6(b).

In general, the most striking feature of SCC is the planar nature of the fracture surfaces, and fiber fracture surfaces that undergo SCC failure show the mirror, mist and hackle regions as shown in Fig. 6(a). These features, however, are not frequently, observed. In this study, it was found that SCC occurs easily in GFRP as the pH concentration of synthetic sea water increases. This implies that chemical attack of the reinforcing fiber is increased with pH concentration of synthetic sea water, and this is based on the fact that glass fibers are rapidly corroded when the

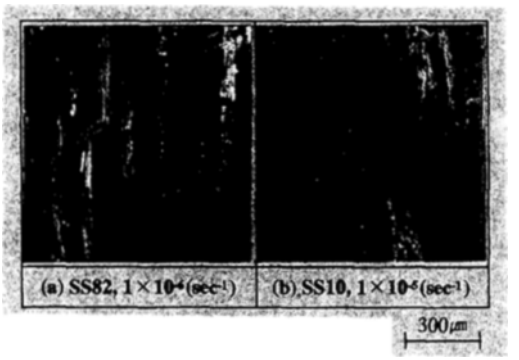

Fig. 9 Stess corrosion fracture surfaces of GFRP tested in synthetic sea water.

concentration of OH^- is in a range from pH9.5 to pH10.0 (Schmitz and Metcalfe, 1966 ; Ishai, 1975).

In the CSM/polyester used in this study, the stress corrosion phenomenon produces partially characteristic planar fractures as shown in Fig. 9. Obviously, if bundles of fibers lie parallel to the fracture plane, then fractures may deviate along the fiber-resin interface. However, fibers inclined at small angles to the fracture plane fail co-planar with minimal pull-out, as shown in Fig. 9.

4. Conclusions

We have investigated the SCC mechanism and the properties of corrosion fracture surface of CSM/polyester composites in sea water. The results obtained through this study are as follows;

(1) For the GFRP used in this study, the hardening of resin in sea water decreases ductile behavior right before fracture, and deterioration of mechanical properties of GFRP results from the loss of interfacial strength in sea water.

(2) The chemical attack of glass fiber is intensified by increasing the pH concentration, and this increases the probability of SCC occurrence.

(3) The chemical attack of glass fiber is intensified by a slow-down in the strain rate because sea water absorption of GFRP through the fiber-resin interface is increased.

(4) The CSM type E-glass/polyester composite tested under particular conditions shows evidence of SCC such as co-planar, mirror and hackle zone.

References

ASTM D 570, 1981, "Standard Test Method for Water Absorption of Plastics," *Annual Book of ASTM Standards,* Vol. 8.01.

ASTM D 1141, 1975, "Standard Specification for Substitute Ocean Water," *Annual Book of ASTM Standards,* Vol. 8.01.

Aveston, J., Kelly, A. and Sillwood, J. M., 1980, "Long Term Strength of Glass Reinforced Plastics in Wet Environments," *Advances in Composite Materials(Bunsell, A. R.),* Pergamon Press, Oxford, pp. 556~568.

Bonniau, P. and Bunsell, A. R., 1981, "Water Absorption by Glass Fiber Reinforced Epoxy Resin," *Composite Structures(Marshall, I. H.),* Applied Science Publishers, London and New Jersey, pp. 92~105.

Dudgeon,C.D.,1987,"PolyesterResins," *Composites, Engineered Materials Handbook(Edited by Reinhart, T. J.), Metals Park,* Ohio, pp. 90~96.

Ishai, O.,1975, "Environmental Effects on Deformation, Strength and Degradation of Unidirectional Glass Fiber Reinforced Plastics," *Polym. Eng. Sci.,* Vol. 15, No. 7, pp. 486~490.

JIS K 7054, 1987, "Testing Method for Tensile Properties of Glass Fiber Reinforced Plastics," *Japanes Industrial Standard.*

Milewski, J. V. and Katz, H. S., 1987, *Handbook of Reinforcements for Plastics,* Van Nostrand Reinhold, New York, pp. 267~275.

Schmitz, G. K. and Metcalfe, A. G., 1966, "Stress Corrosion of E-glass Fibers," *Ind. Eng. Chem., Res. & Dev.,* Vol. 5, No. 1, pp. 1~8.